

Supporting Information for

Ti³⁺ Self-Doping in BaTiO₃ Ceramic for Multi-Sensor Applications: Reduced Bandgap with Maintained Ferroelectric Properties

Chen Xi Li^{ab}, Xiang Li^{ab}, Xin Yi Chen^b, Chen Chen^c, Lei Zhao^{a*} and Nan Ma^{b*}

^a Key Laboratory of High-precision Computation and Application of Quantum Field Theory of Hebei Province, College Physics Science and Technology, Hebei University, Baoding, 071002, China

E-mail: leizhao@hbu.edu.cn

^b CAS Key Laboratory of Inorganic Functional Materials and Devices, Shanghai Institute of Ceramics, Chinese Academy of Sciences, Shanghai, 201899, China. E-mail: manan@mail.sic.ac.cn

^c State Key Laboratory of High Performance Ceramics and Superfine Microstructure, Shanghai Institute of Ceramics, Chinese Academy of Sciences, Shanghai, 201899, China

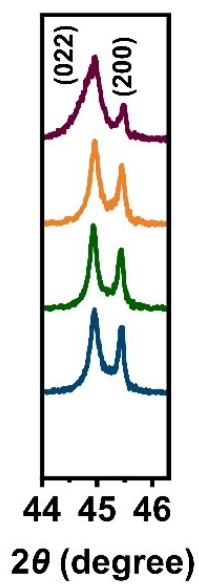


Figure S1 Enlarged XRD patterns around 45° .

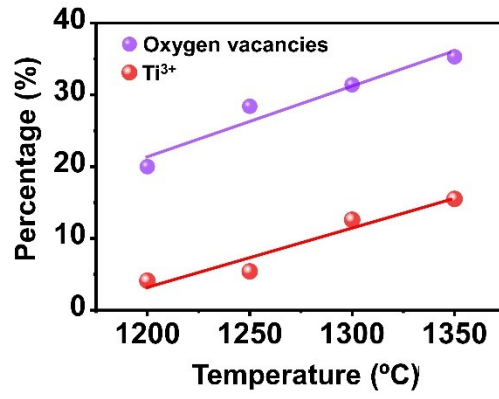


Figure S2 Sintering temperature dependence of the concentration of oxygen vacancies and Ti³⁺.

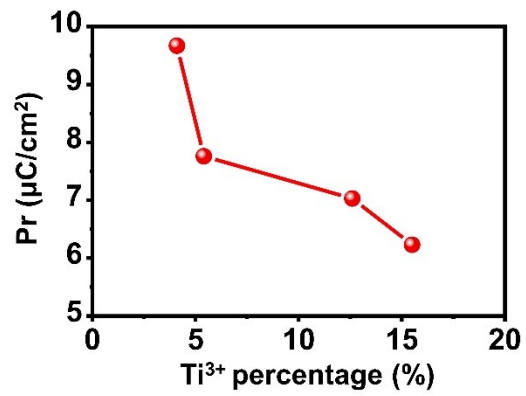


Figure S3 Change of P_r as a function of the amount of Ti^{3+} .

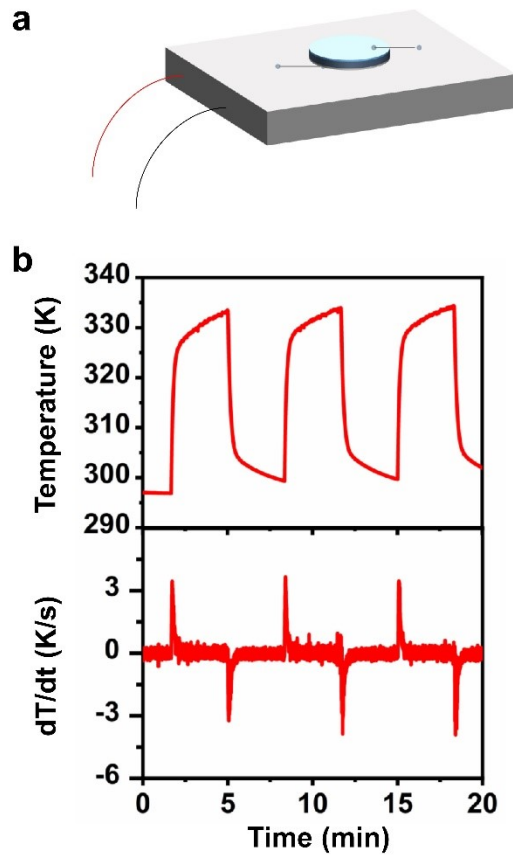


Figure S4 (a) Schematic illustration of the pyroelectric current measurement; (b) The periodic temperature change and the corresponding temperature change rate.

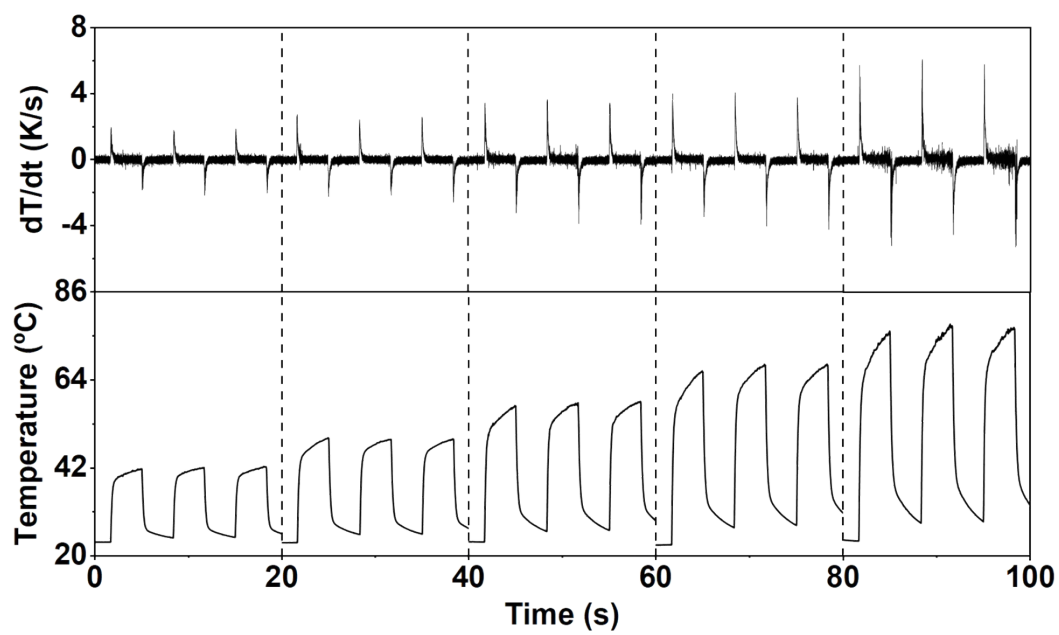


Figure S5 Temperature change and the corresponding change rates.

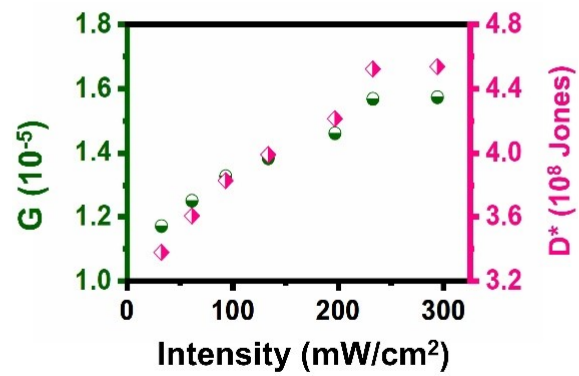


Figure S6 Light intensity-dependent of photoconductive gain G and specific detectivity D^* .

Table S1 Binding energy of different temperature-sintered BTO samples.

	O_L	O_V	O_{ads}	Ti³⁺ 2p3/ 2	Ti³⁺ 2p1/ 2	Ti⁴⁺ 2p3/ 2	Ti⁴⁺ 2p1/ 2
1200 °C	529.0	530.8	531.8	457.6	463.0	457.9	463.7
1250 °C	529.1	530.9	532.0	457.7	463.1	458.0	463.8
1300 °C	529.2	530.9	532.2	457.8	463.3	458.2	464.0
1350 °C	529.2	531.0	532.4	457.8	463.5	458.2	464.0

Table S2 Comparison of the Photodetection Parameters for Ti³⁺-BTO Photodetector and Other Ferroelectric Materials Based Self-powered Photodetectors.

Photodetector	Working Mechanism	Wavelength h (nm)	R (A/W)	D* (Jones)
¹ BaTiO ₃	Photovoltaic-pyroelectric	405	3.25×10 ⁻⁷	2.97×10 ⁵
² BaTiO ₃	Photovoltaic	405	3.5×10 ⁻⁷	1.1×10 ⁶
³ BiFeO ₃	Photovoltaic-pyroelectric	450	2.4×10 ⁻⁷	8.5×10 ⁸
⁴ Bi _{0.5} Na _{0.5} TiO ₃	Ferro-pyro-phototronic	405	4.06×10 ⁻⁶	1.27×10 ⁷
⁵ PLZTN9	Ferroelectric photovoltaic	AM 1.5G	3.67×10 ⁻⁷	9.08×10 ⁷
⁶ BZT-BCT	Photovoltaic-pyroelectric	405	8.48×10 ⁻⁷	2.37×10 ⁶
⁷ PLZT	FE polarization and Schottky barrier	340	1.12×10 ⁻⁵	4.43×10 ⁸
Ti ³⁺ Self-doped BaTiO ₃ (This work)	FE polarization and Schottky barrier	405	5.14×10 ⁻⁶	4.54×10 ⁸

References for Supporting Information

- [1] N. Ma and K. Zhang, Y. Yang, *Adv. Mater.* 2017, **29**, 1703694.
- [2] N. Ma and Y. Yang, *Nano Energy*, 2018, **50**, 417-424.
- [3] J. Qi, N. Ma and Y. Yang, *Adv. Mater. Interfaces*, 2018, **5**, 1701189.
- [4] Y. Liu, Y. Ji, Y. Xia, L. Wu, C. R. Bowen and Y. Yang, *Nano Energy*, 2022, **98**, 107312.
- [5] G. Huangfu, H. Xiao, L. Guan, H. Zhong, C. Hu, Z. Shi and Y. Guo, *ACS Appl. Mater. Interfaces*, 2020, **12**, 33950-33959.
- [6] L. Wang, C. Chen, X. He, K. Yao and Z. Yi, *J. Am. Ceram. Soc.*, 2023, **106**, 389-398
- [7] J. Chen, A. S. Priya, D. You, W. Pei, Q. Zhang, Y. Lu, M. Li, J. Guo and Y. He, *Sens. Actuators A Phys.*, 2020, **315**, 112267